We are IntechOpen,
the world's leading publisher of Open Access books
Built by scientists, for scientists

4,800
Open access books available

122,000
International authors and editors

135M
Downloads

154
Countries delivered to

Our authors are among the

TOP 1%
most cited scientists

12.2%
Contributors from top 500 universities

CLARIVATE ANALYTICS
BOOK CITATION INDEX
INDEXED

WEB OF SCIENCE™

Selection of our books indexed in the Book Citation Index
in Web of Science™ Core Collection (BKCI)

Interested in publishing with us?
Contact book.department@intechopen.com

Numbers displayed above are based on latest data collected.
For more information visit www.intechopen.com

Controlled Post-treatment of Thick CVD-Diamond Coatings by High-Density Plasma Oxidation

Tatsuhiko Aizawa

Abstract

CVD-diamond coatings were posttreated by plasma oxidation to recycle an original WC (Co) mother tool substrate for recoating and reuse. A developed RF/DC plasma oxidation system was stated together with a hollow cathode device to intensify the oxygen ion and electron densities and with a quantitative plasma diagnosis equipment. Plasma oxidation ashing conditions were optimized by this quantitative diagnosis toward the perfect ashing of diamond films with less residuals and less tool edge damage. Geometric effect of tool teeth structure on this ashing process was discussed by in situ monitoring of plasmas. Engineering solution of this ashing process was proposed for industrial applications.

Keywords: plasma oxidation, CVD-diamond coating, ashing, hollow cathode device, quantitative plasma diagnosis

1. Introduction

CVD-diamond coatings as well as poly-crystalline diamonds have been widely utilized for the protection of dies and tools from wear and damage in cutting, drilling, and piercing operations in practice [1]. They are also expected to be working as a semi-conductive and thermal-conductive substrate for micro-electro-mechanical system (MEMS) and Bio-MEMS [2]. In parallel with high qualification in CVD-diamond coating technologies, how to make accurate shaping, micro–/nano-texturing, polishing and finishing of diamond films also becomes an engineering issue [3].

In the literature of patents to search for qualification in ashing the used diamond coatings, many studies have been developed to efficiently remove the diamond films from WC (Co) (Tungsten Carbide with Cobalt binder) and silicon substrates. Among them, three ashing processes were

noticed; the laser machining [4], the ion-beam and plasma discharging [5], and the reactive etching method [6]. The former two methods are difficult to be applied to tools with complex shaped teeth. Residuals of diamond were left on the treated tool surface. WC (Co) substrate suffered from severe thermal and chemical transients. Plasma oxidation method [7] has grown up as one of the most promising approaches to ashing. The CVD-diamond films are physically or chemically removed by ion bombardment and/or plasma-driven chemical reactions. These plasma ashing processes encounter some severe practical difficulties: (1) imperfect ashing of diamond films, (2) long leading time, (3) residual diamond films, especially behind the cutting teeth, (4) overoxidation of WC (Co) substrate, and (5) damage at cutting tooth edges. The used carbon-base coatings were removed from substrates by nontraditional plasma oxidation method for industrial application [8–11]. In this chapter, RF/DC plasma oxidation system with hollow cathode devices is introduced as an effective ashing method. Plasma oxidation processing for posttreatment of diamond films is stated with comments on its fundamental features and application to industries. Quantitative plasma diagnosis is utilized to characterize the oxygen plasmas and to describe the ashing process. Two types of CVD-diamond-coated cutting tools are employed as a specimen to demonstrate the effectiveness of present plasma oxidation ashing.

2. Plasma oxidation processing

The glow discharging process is utilized to ignite the oxygen plasmas by the application of radio-frequency (RF) power and direct current (DC) bias. This oxygen plasma density is effectively intensified by using the hollow cathode devices. Emissive light optical spectroscopy (EOS) as well as the Langmuir probe are utilized to quantitatively characterize the oxygen plasma state and to describe the reaction process during oxidation. CVD-diamond-coated tools are prepared for ashing treatments.

2.1. RF/DC plasma oxidation system

Different from the conventional DC- or RF-plasma generators, where plasmas are ignited and generated in the frequency of 13.56 MHz or its multiples, the present RF/DC oxygen plasmas are ignited at 2 MHz without use of matching box, as shown in **Figure 1**.

This frequency is automatically adjusted to keep matching between input and out powers around 2 MHz [7, 12–13]. This automatic and prompt response in power matching stabilizes the temporally varying plasma state. As reported in [7], a longer response time in the order of 1–10 s is needed for the mechanical matching box to adjust the RF-power. The present oxygen plasma state for ashing process is controlled within 1 ms in response; there is no time delay in power control. The vacuum chamber is electrically neutral without a self-biased current. Both the RF-voltage and DC-bias are controlled independently from each other to be from 0 to 250 V, and, from 0 to 600 V, respectively. This RF-plasma is ignited and controlled by using a dipole electrode, while the DC bias is directly applied to the specimens. In the following ashing experiments, the specimens were located on the cathode table before evacuation down to the base pressure. Then, a carrier gas was introduced into the chamber to attain the specified pressure. Both oxygen and argon gases were available in this system besides the nitrogen gas for bent.
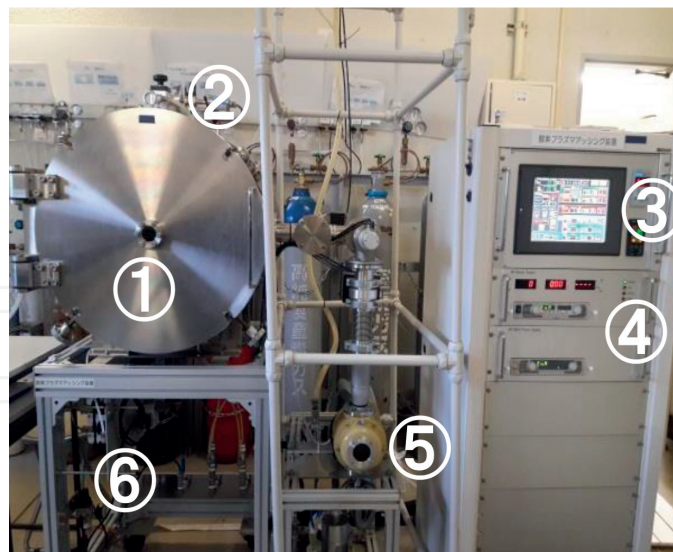
Figure 1. High density RF-DC oxygen plasma etching system. ① vacuum chamber, ② RF-generator, ③ control panel, ④ RF- and DC-power supplies, ⑤ evacuation units, and ⑥ carrier gas supply.

2.2. Plasma oxidation diagnosis

EOS (Hamamatsu Photonics, Co., Ltd., Japan) is first utilized for diagnosis on the oxygen plasmas, as shown in **Figure 2**. The emissive light from plasmas is detected through a silica window of chamber to send the signals to the analyzer via the optical fibers. This spectro-scopic analysis is also useful to make on-line monitoring on plasma state in ashing. Each activated species in the plasma is identified by its corresponding peak at the specified wave length in the measured spectrum. **Figure 2** also illustrates the Langmuir probe, equipped to the present ashing system. Both the ion/electron density and electron temperature are mea-sured for optimization of ashing process. With this information of density and temperature
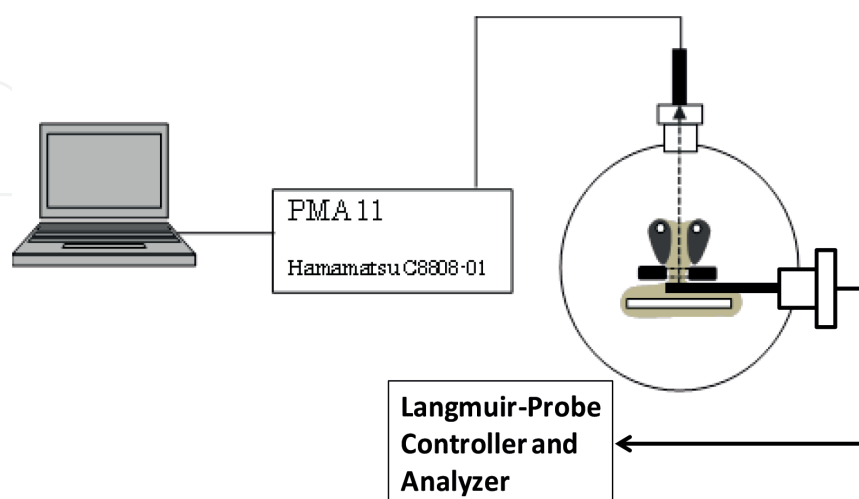
Figure 2. Quantitative plasma diagnosis to measure the electron density and temperature as well as the spectrum of activated species in plasmas.
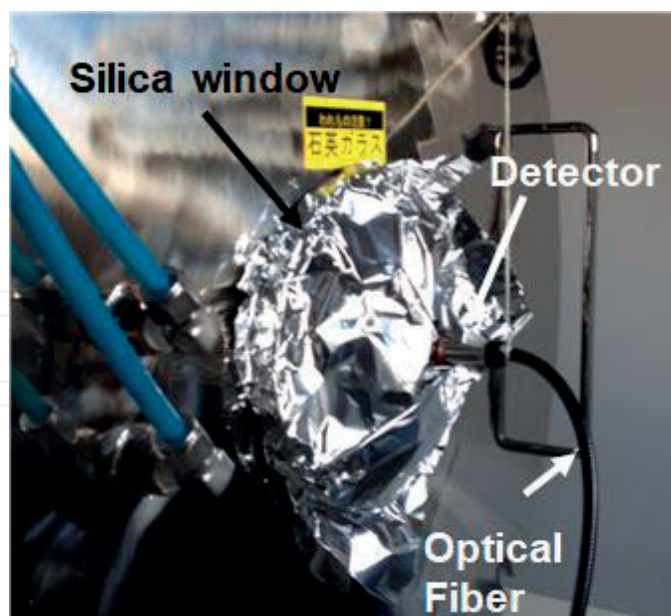
Figure 3. An experimental set-up for plasma diagnosis by EOS.

both for electrons, ions and radicals, the plasma state in processing are precisely defined and described to investigate the effect of plasma processing parameters on the ashing behavior.

Let us first explain the experimental set-up for EOS and measure the typical spectra in the function of oxygen gas pressure [14]. **Figure 3** shows an experimental set-up to make EOS. The whole window was covered by a pure aluminum sheet to be free from noises. The measuring point can be varied by focusing; the plasma state at the focused point in the chamber is in situ measured during oxidation process.

When RF voltage was 250 V and DC-bias, −500 V, the emissive light optical spectra were measured in the function of gas pressure. As shown in **Figure 4**, the oxygen molecular ion O_2^+ as well as the oxygen ion (OII or O^+) has the highest peak at 774 and 470 nm, respectively.

The intensity of oxygen ions (OI or O^*; OII or O^+; OIII or O^{2+}) and O_2^+ reduced with increasing the gas pressure in **Figure 4**. This is because the reaction cross-section significantly reduces for electron detachment from oxygen molecules.

The Langmuir probe is employed to measure the electron and ion densities as well as the electron temperature. The experimental set-up for I-V curve measurement in the RF/DC plasmas is depicted in **Figure 5**. The accuracy in measurement strongly depends on the tip geometry and resistivity; e.g., the tip radius is 350 μm, the tip holder, 3 mm, the probe tip length, 1 cm, and, the tip resistance, 36 Ohm, as shown in **Figure 5(b)**.

The measured I-V curve is nearly constant but abruptly changes at the vicinity of plasma potential. This I-V curve is deconvoluted to deduce each contribution of ions and electrons to measured current density. Each I-V curve for ion and electron is differentiated to calculate its first and second derivatives across the plasma potential; the electron and ion density as well as the electron temperature are deduced from this direct calculation. **Figure 6** depicts the variation of measured ion density with the oxygen gas pressure when the DC bias was −600 V. Reduction of ion density
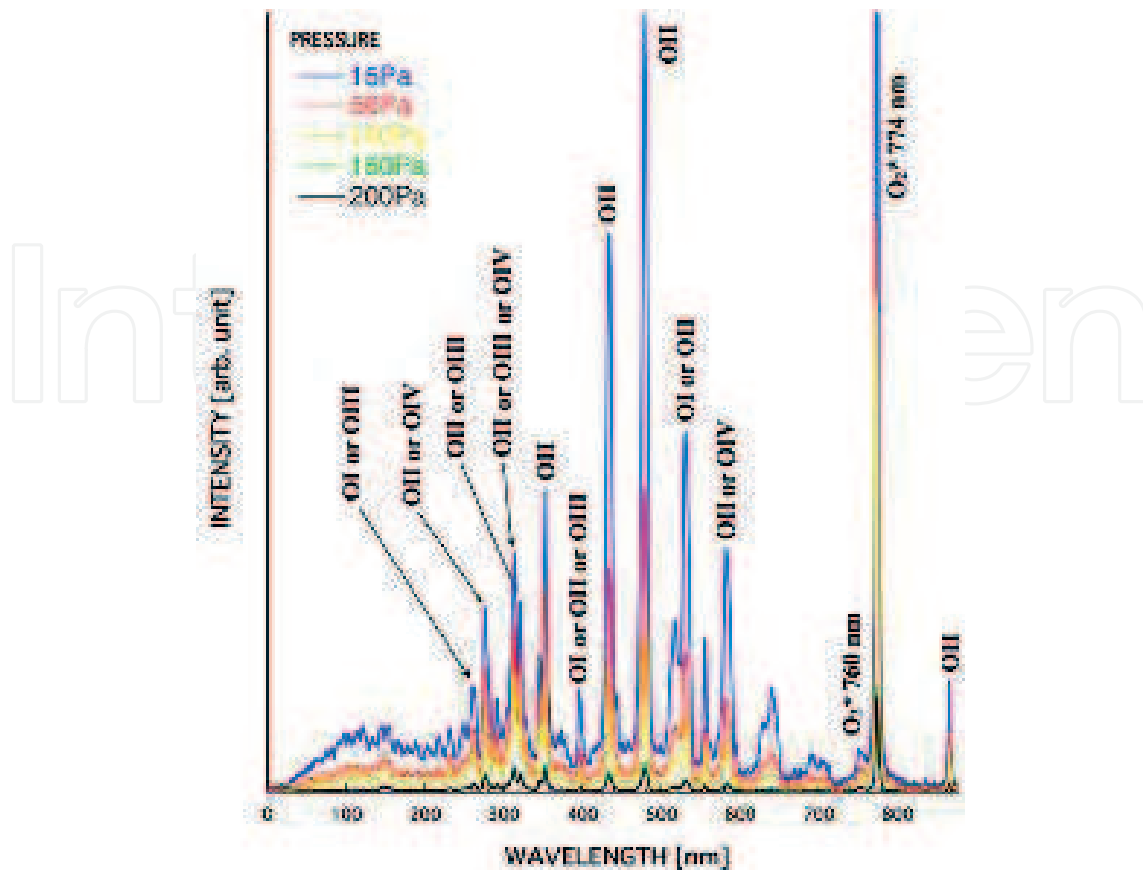
Figure 4. Measured emissive light optical spectra in the function of gas pressure for a standard RF/DC plasma under [250 V; −500 V].
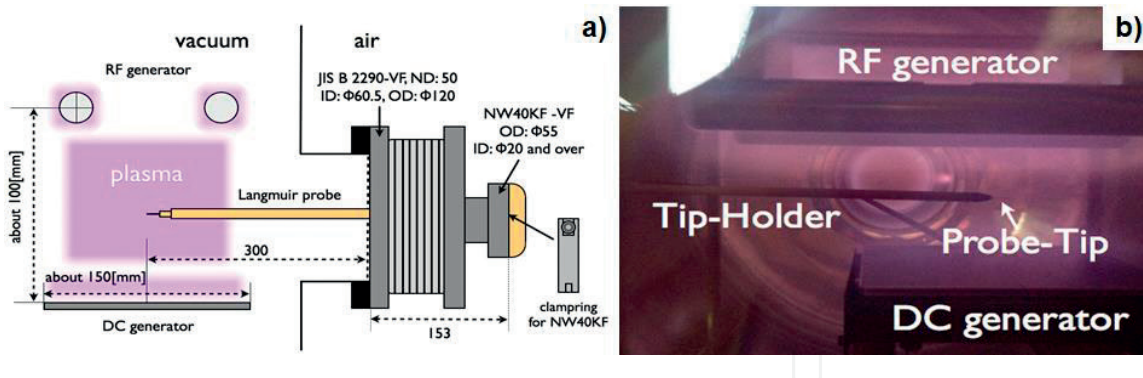
Figure 5. Experimental set-up for measurement of ion and electron densities as well as electron temperature at the specified position in the RF/DC plasmas by using the Langmuir probe.

was only measured in the range of 150–175 Pa; ion density monotonically increases with the pressure when DC bias was more than −500 V. Ionization is activated with increasing the pressure because of collision of electrons with oxygen molecules. Finally, the present RF/DC plasma characteristics is compared with the ICP (Induction-Coupled Plasma) where a cylindrical tube with diameter 40 mm and a length of 600 mm was used to ignite the plasmas. At the pressure of 75 Pa, the electron density (N_e) reaches to 4.8×10^{16} m^{-3} with the electron temperature (T_e) of 3.9 eV in
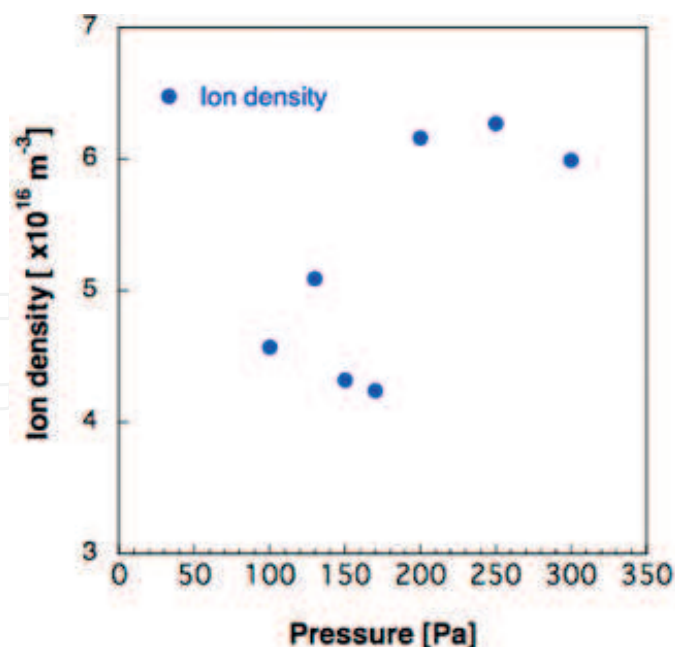
Figure 6. Variation of the measured ion density with the gas pressure by the Langmuir probe.

the present system. When using ICP, Ne = 1.0 × 10^{16} m^{-3} and Te = 5.0 eV in [15]. Higher electron density by five times can be attained even at the center of large chamber in **Figures 1** and **5(b)**.
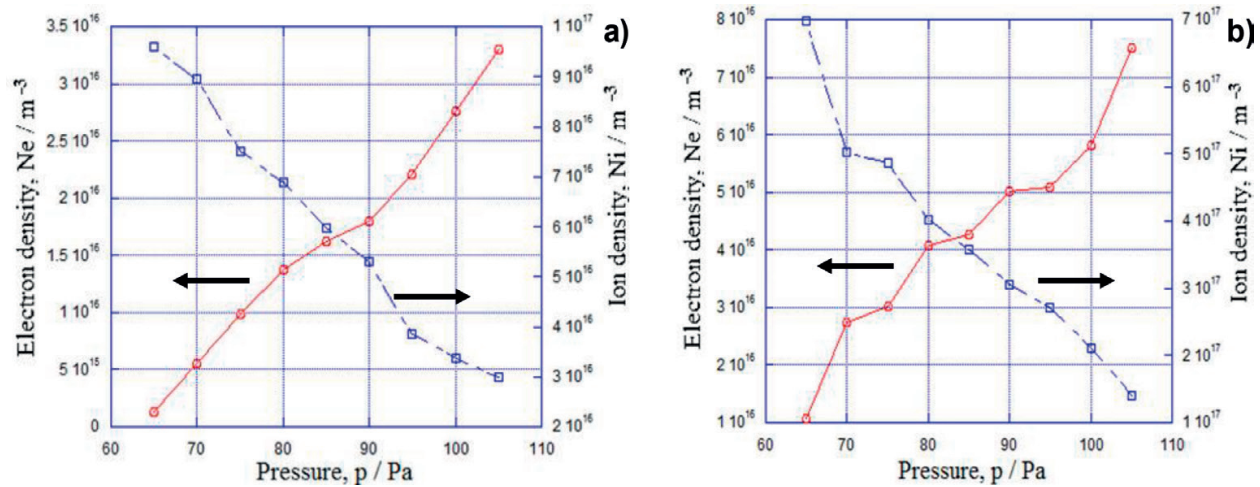
2.3. High-density plasma oxidation

Various tools and devices are available to intensity ion and electron densities in the plasmas. A magnetism works as a lens to concentrate the ions in the magnetic field [16, 17]; ion density increases with increasing the magnetic field strength. Electric insulation is also effective to separate the plasmas into the specified spaces [18]. In this study on the plasma oxidation, a hollow cathode device [19] is selected and redesigned to confine the oxygen plasmas in the hollow and to intensity their ion and electron densities. The quantitative plasma diagnosis in 2.2 is also utilized to describe how much the oxygen ion and electron densities are enhanced by the hollow cathode device.

Variation of the electron and oxygen ion densities with pressure is compared in **Figure 7** without and with use of the hollow cathode. At the pressure of 75 Pa, N_i = 7.8 × 10^{16} m^{-3} in **Figure 7(a)**; this N_i is enhanced to be 5 × 10^{17} m^{-3} when using the hollow cathode device in **Figure 7(b)**. In the following, this hollow cathode device is redesigned to make effective ashing of diamond films coated on the cutting and end-milling tools.

2.4. Observation and measurement

High resolution optical microscopy as well as scanning electron microscopy (SEM) are utilized to observe the ashed surfaces of diamond-coated specimens. Raman spectroscopy is also used to detect a characteristic peak to the diamond.

Figure 7. Comparison of the ion and electron density variation with pressure with and without use of the hollow cathode device. (a) RF-DC plasmas in **Figure 1** without use of the hollow cathode, and, (b) with use of the hollow cathode.

3. Plasma oxidation ashing of used diamond films

Plasma oxidation ashing process is employed to make perfect removal of used diamond films, coated onto the WC (Co) cutting tools, with minimum damage to tool teeth and to recycle the mother WC (Co) substrate for recoating and reuse. As an engineering issue, no residuals of diamond films are left on the WC (Co) substrate, less damage is induced during ashing process, and, this ashing must be done in short duration.

3.1. Background

CVD-diamond-coated WC (Co) cutting, drilling, and end-milling tools have been widely utilized for dry machining of the carbon fiber–reinforced plastic (CFRP) or Carbon fiber–reinforced thermoplastic (CFRTP) components and parts in the airplanes and automobiles [20, 21]. These materials are used for main cabin and wings; a hundred thousand holes must be machined or drilled into these CFRP/CFRTP structural members for each airplane in dry by using the diamond-coated tools. Since the number of airplanes is expected to be doubled in next 8 years, the above tooling cost percentage significantly increases in the total production cost. Event at present, the carbon fibers in CFRP/CFRTP have high strength and stiffness enough to make fatal damage and defect to the diamond coating of machining tools. Since an equivalent number of holes to be machined are estimated to be 100,000 per an airplane, the production cost, especially the tooling cost, increases with demanded numbers of planes or cars. Those new materials are too hard to machine or drill without damages to CVD-diamond-coated WC (Co) tools; the used tool is exchanged with new one in every machining by 10 m, or in every drilling by 10 holes [22]. How to recycle the WC (Co) substrate is essential to reduce the cost.

These used or damaged diamond coatings must be once removed to recycle the WC (Co) tool substrate with less damages to its tooth geometry before recoating and to reuse this in cutting operations. RF/DC plasma oxidation process was demonstrated to be useful for perfect

removal of used tetragonal amorphous carbon coating or t-a:C coatings and for recycle of WC (Co) cutting substrate [23–25]. The recoated WC (Co) tools were proven to have the same capability in cutting performance as the virgin tools [24, 25]. This plasma oxidation process is further advanced to remove the used diamond coatings for recycle and reuse and to reduce the production cost in machining of CFRP/CFRTP members [26–28].

3.2. Preparation of diamond-coated tools

The diamond-coated WC (Co) end-milling tools were prepared for ashing experiments. As shown in **Figure 8**, two types of tools were employed to investigate the effect of tooth geometry on the plasma ashing process. The tool with the length of 70 mm, the diameter of 10 mm, and the edge skew angle of 30° was used as a standard specimen to search for an optimum ashing condition. A small-sized tool with the length of 70 mm, the diameter of 6 mm, and the edge skew angle of 10° was also used to investigate whether the optimal ashing condition is affected by down-sizing. The diamond film thickness was common in both tools by 15 μm.
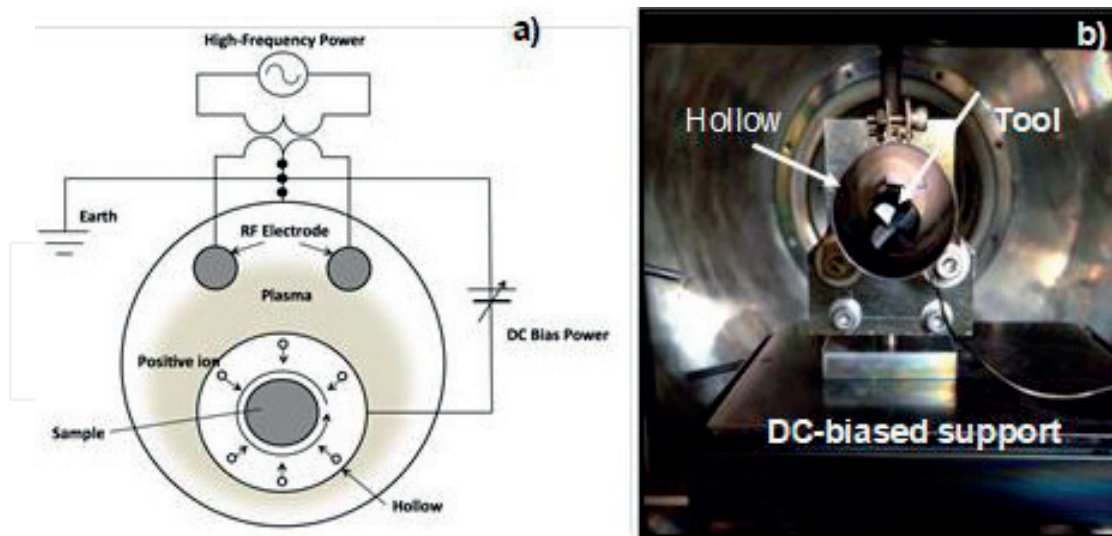
3.3. Experimental set-up

An end-milling tool has skewed tooth geometry; diamond films are coated even on the curved surfaces backward the teeth. A special hollow cathode is designed to preserve the confined plasma in the hollow against the rotating tools. **Figure 9** depicts the developed hollow cathode device for ashing.

The generated RF-plasma is confined in this hollow so that higher ion and electron densities are attained for ashing the diamond films. As shown in **Figure 9(a)**, a diamond-coated tool is placed in the center of hollow tube; the same DC-bias is applied to both the hollow and the tool. Although the rotating speed has influence on the plasma configuration, it is selected to be 6 rpm in the following experiments.

A standard experimental set up is summarized as follows. After placing the specimen in **Figure 9(b)**, the chamber is evacuated down to the base pressure, less than 5×10^{-3} Pa. The pure oxygen gas with its purity of 99.99% is introduced as a carrier gas. RF- and DC- bias voltages

Figure 8. Two diamond-coated end-milling tools as a specimen for plasma ashing process.

Figure 9. Special hollow cathode device for ashing the diamond films on the WC (Co) end-milling tool substrate. (a) Illustration of hollow cathode device, and, (b) experimental set-up for ashing.

are variable from 100 to 250 V and from −400 to −800 V, respectively. The plasma pressure (p) is marginable to be determined; in the following, $25 < p < 100$ Pa. The plasma oxidation conditions are optimized by the quantitative plasma diagnosis to be 100 V for RF-voltage, −500 V for DC-bias, 45 Pa for pressure and 3.6 ks for duration time.

3.4. Experimental results

A standard specimen is first employed to investigate the effect of plasma processing parameters on the ashing behavior. Under the optimal conditions, the small-scaled tool specimen is also used to describe the geometric effect of tool teeth on the ashing process. Difference in ashing process conditions is explained by the in situ plasma diagnosis.

3.4.1. Standard end-milling tools

Both RF-voltage and pressure are varied to describe the plasma ashing process. In the first experiment, RF-voltage was set to be 250 V, DC-bias, −650 V and oxygen gas pressure, 30 Pa. **Figure 10** shows the ashed specimen for 3.6 ks.

Since cobalt in WC (Co) is mainly oxidized, the tool surface is colored in green in **Figure 10(a)**. No residual diamond debris are left on the tool surface in **Figure 10(b)**. Due to this excess in oxidation, the shrinkage of tool edge reaches to 7.7 μm in **Figure 10(c)**. In order to reduce the oxidation rate, the above processing parameters are tuned to be (250 V; −500 V; 45 Pa; 3.6 ks). **Figure 11** depicts the surface condition and SEM image of ashed specimen.

The surface is colored in reddish yellow in **Figure 11(a)**; this implies that a part of tungsten in WC (Co) is mainly oxidized even under this condition. Almost all the diamond films are removed on the tool surface in **Figure 11(b)**. This over-oxidation results in a significant shrinkage of edge by 9.7 μm in **Figure 11(c)**. To be discussed in later, the activated oxygen atom density must be directly controlled by lowering the RF-voltage.

Figure 12(a) depicts the ashed tool surface by lowering the RF-voltage down to 100 V. No oxide layers of cobalt and tungsten are seen on the WC (Co) substrate surface. The original diamond
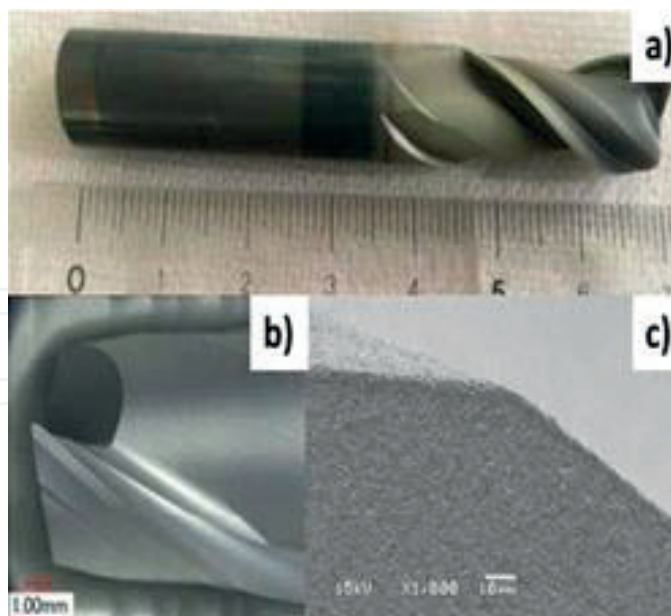
Figure 10. Ashing of CVD-diamond coating on the WC (Co) standard specimen under (250 V; −650 V; 30 Pa; 3.6 ks). (a) Surface of ashed specimen before cleansing, (b) Ashed tool edge, (c) SEM image of tool edge.
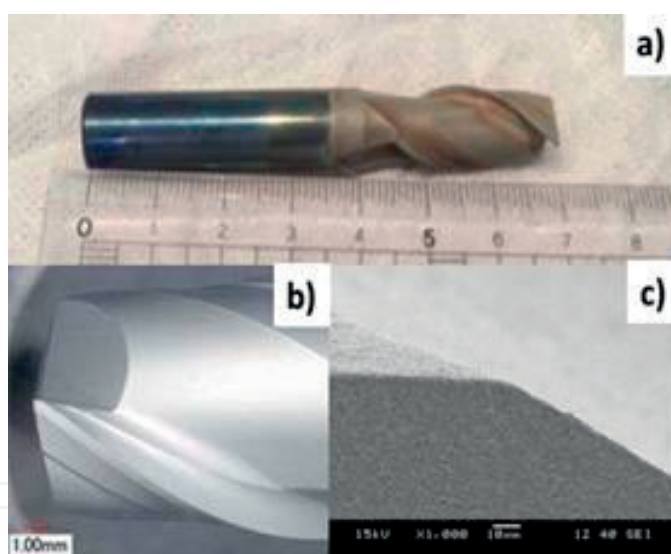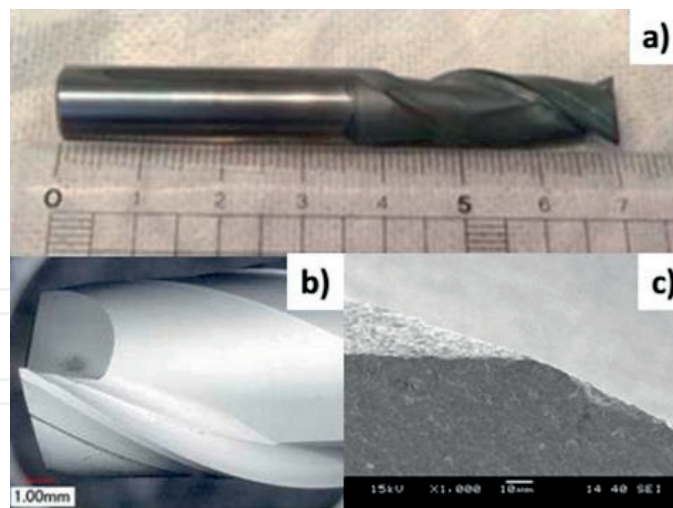

Figure 11. Ashing of CVD-diamond coating on the WC (Co) standard specimen under (250 V; −-500 V; 45 Pa; 3.6 ks). (a) Surface of ashed specimen before cleansing, (b) Ashed tool edge, (c) SEM image of tool edge.

coatings are completely removed only after ashing for 3.6 ks, as shown in **Figure 12(b)**. The shrinkage of tool edge is limited by 1.1 μm in **Figure 12(c)**. Fine SEM observation and the Raman spectroscopy are utilized to precisely describe this ashing process. **Figure 13** compares the top view in SEM image for the WC (Co) tool surface before and after ashing under this optimal condition of (100 V; −-500 V; 45 Pa; 3.6 ks).

The original tetrahedral diamond crystals with significant roughness in **Figure 13(a)** are completely removed to leave a flat WC (Co) surface with micro-pores among WC grains. These

Figure 12. Ashing of CVD-diamond coating on the WC (Co) standard specimen under (100 V; −500 V; 45 Pa; 3.6 ks). (a) Surface of ashed specimen before cleansing, (b) Ashed tool edge, (c) SEM image of tool edge.
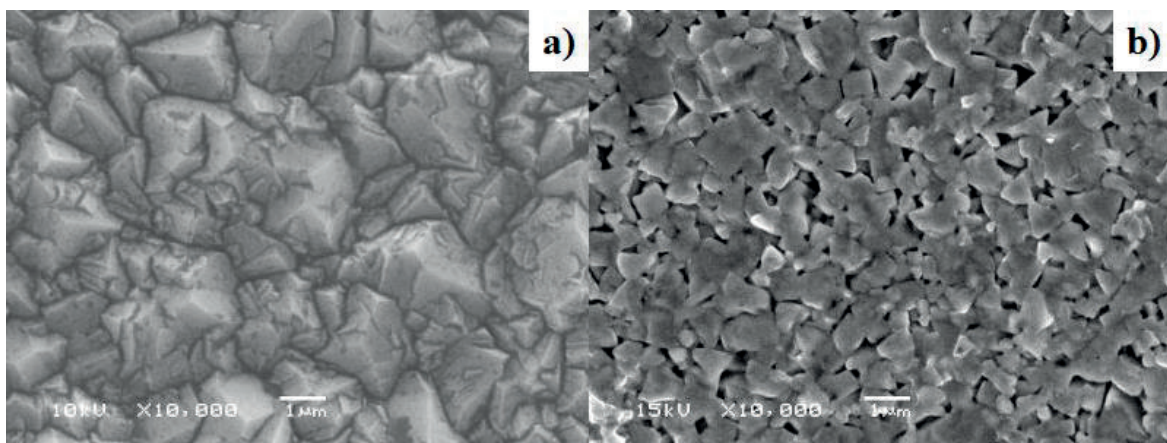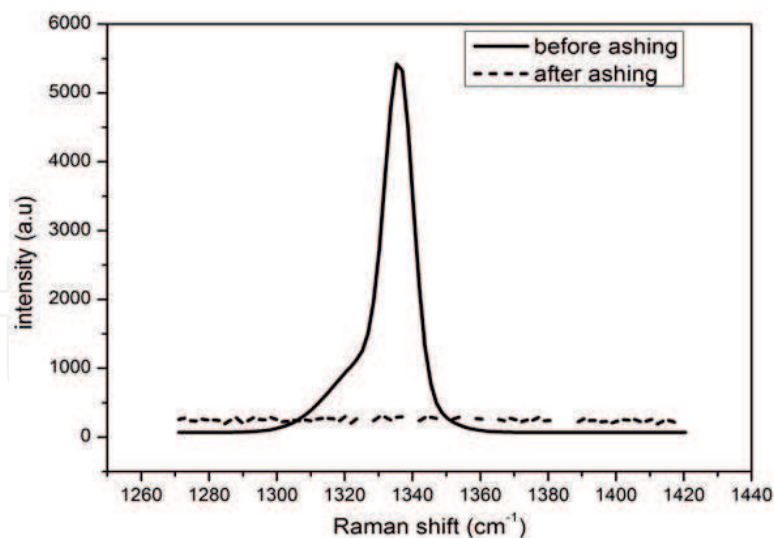

Figure 13. Comparison of microstructure on the diamond-coated tool surface before and after ashing under (100 V; −500 V; 45 Pa; 3.6 ks). (a) before ashing, and, (b) after ashing.

micro-pores are accommodated as a nucleation site for diamonds by selective removing the cobalt binders before CVD-coating. Hence, this microstructure in **Figure 13(b)** proves that starting WC (Co) substrate surface before coating is reproduced by the present ashing process. The Raman spectroscopy is also utilized to precisely check whether a residual debris of diamond is left on the ashed tool surface. **Figure 14** compares the Raman spectra before and after ashing. The presence of diamond film is identified by the Raman peak around 1330 cm^{-1} as shown in **Figure 14**. No peaks are detected at the vicinity of 1330 cm^{-1} in **Figure 14** after ashing; no diamond residuals are left on the tool surface after ashing.

3.4.2. Small-scaled end-milling tools

The small sized tools, as shown in **Figure 8**, were posttreated by plasma oxidation under the optimum condition in the above, or, (100 V; −500 V; 45 Pa; 3.6 ks). High resolution optical

Figure 14. Comparison of the Raman spectra for the diamond-coated tool surface before and after ashing under (100 V; −500 V; 45 Pa; 3.6 ks).
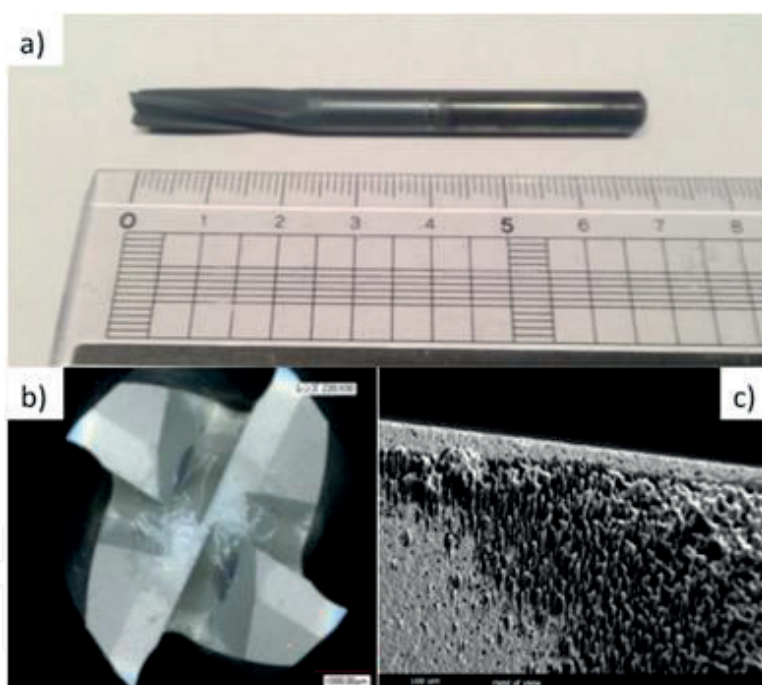
Figure 15. Ashing of CVD-diamond coating on the WC (Co) small-scaled specimen under (250 V; −500 V; 45 Pa; 3.6 ks). (a) Surface of ashed specimen before cleansing, (b) Ashed tool edge, (c) SEM image of tool edge.

microscopy and SEM are also utilized to make close observation on the ashed surfaces of small sized tools. As shown in **Figure 15(a)**, the outlook color of ashed tooth surfaces is gray in the similar manner to **Figure 12(a)**. **Figure 15(b)** shows the top tooth surfaces of ashed tools. No diamond films are left on the surfaces. These prove that most of diamond films coated on the small sized tools are also homogeneously removed just in correspondence to **Figure 12(b)** for the standard tool. After close observation on the whole tooth surfaces by SEM, a cold spot with the residual diamonds was detected on the rake face or the gash of tools. A typical SEM image is shown in **Figure 15(c)**. The diamond films at the upper edge and on the left-hand

surface are almost completely ashed away; the diamond residuals are left as a dendritic column with the average diameter of 5–10 μm.

This difference in ashing behavior between two specimens comes from the optimality in oxygen plasma sheath distribution surrounding the tool surface. The plasma diagnosis is also employed to describe this effect of the plasma state on the ashing behavior.

3.4.3. In situ plasma diagnosis

EOS works to monitor the temporal variation of oxygen plasma state during the ashing process. Since the carbon in diamond reacts with oxygen atom, a peak for resultant of CO by the reaction, C (in diamond) + O (from O* and O^+ in palsmas) -> CO, is detected by EOS together with oxygen-related peaks. Hence, in this in situ EOS-diagnosis, oxygen peak at 470 nm and CO-peak at 288 nm are monitored to describe the plasma reaction for ashing.

Figure 16 depicts a time evolution of measured O- and CO-peak intensities by this in situ EOS. O-peak intensity is constant during ashing process; a constant oxygen atom flux is supplied to hot spots of plasma reaction. CO-peak intensity is enhanced in the early stage in ashing; it exponentially decays from t = 1000 s to be lower level and nearly minimum for t = 4000 s. This implies that homogeneous ashing process retards by itself with a constant time exponent. Hence, this exponential decay of CO-peak intensity with time proves that the diamond coating is homogeneously ashed away.

This time transient of CO-peak intensity is employed to describe the difference in ashing behavior between two diamond-coated tools. When using the standard tool, two CO-peak intensities, monitored at λ = 287 and 312 nm, exponentially decrease with time as shown in **Figure 17(a)**. Just as seen in **Figure 16**, the diamond film is expected to be homogeneously ashed away from this in situ diagnosis. This homogeneous ashing has been proven by precise observation on the posttreated tool surfaces as shown in **Figures 12–14**. On the other
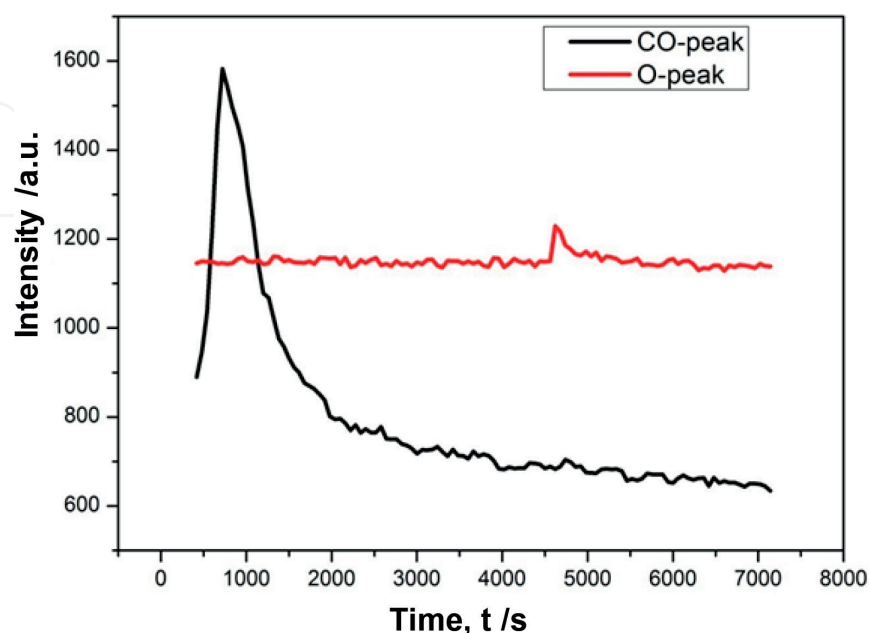
Figure 16. Temporal evolution of O- and CO-peak intensities, measured by the in situ EOS.
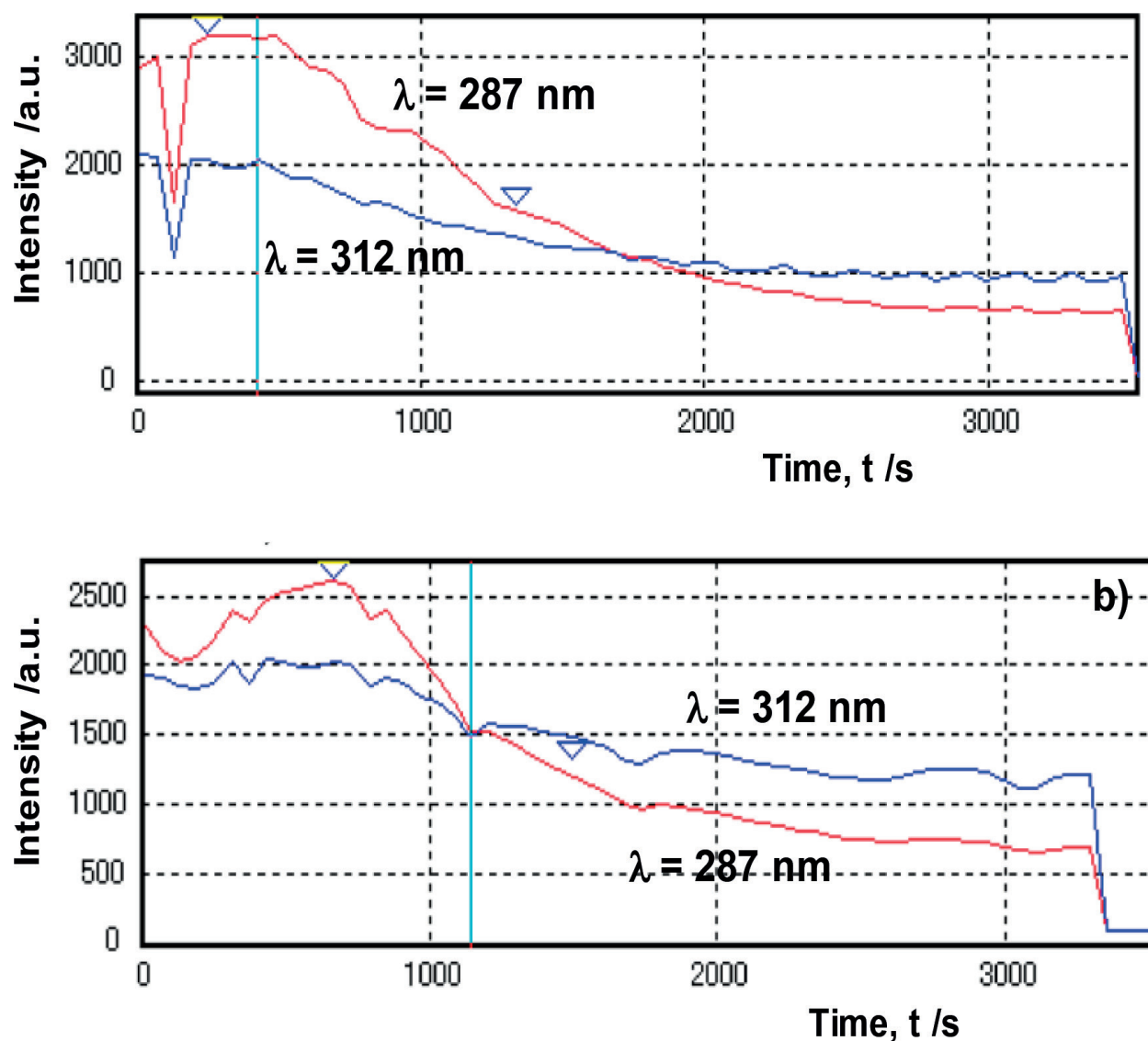
Figure 17. Time transients of CO-peak intensities at λ = 287 and 312 nm by the EOS in situ monitoring during ashing process.

hand, when using the small-sized tool, this time transient changes by itself as depicted in **Figure 17(b)**. The up-and-down deviation of CO-peak intensity reveals that ashing reaction localizes in hot spot at one surface but in cold spot at other surfaces. This heterogeneous ashing process results in a residual diamond film at the cold spots such as a small part on the rake edges of tools as shown in **Figure 15(c)**.

3.5. Summary

A diamond film coated onto a single WC (Co) tool substrate in a standard size was successfully ashed away without residuals and with much less damage at the tool tooth-edges. Due to this perfect ashing of diamond films, an original WC (Co) substrate surface was reproduced to have a decobalted WC (Co) microstructure. This posttreated surface is easy to be diamond-recoated for reuse of tools. The duration time for this ashing is only 3.6 ks, much faster than

the commercial operation time by 20–30 hours experienced in several tooling companies. The whole ashing process can be in situ controlled by monitoring the CO-peak intensities at the specified wave length through EOS. A homogeneous, perfect ashing is guaranteed by an exponential decay of CO-peak intensity with time in this quantitative diagnosis. The tool teeth-edge geometry has significant effect on the formation of plasma sheaths on the tool surfaces. Inhomogeneous ashing can be also detected by the in situ plasma diagnosis; plasma oxidation conditions must be tailored for each tool geometry in practice.

4. Discussion

How to design this asbing process in practice and how to apply this posttreatment to industries are discussed in this session.

4.1. Plasma processing design

Theoretical plasma processing design is often needed to construct a new device to control a plasma configuration in chamber and to understand the experimental results [29]. Some studies have just started to build up this theoretical model. Among them, for an example, the Boltzmann equation was solved to obtain electron transport coefficients and rate coefficients for fluid models [30].

In the present study, a multi-disciplinary program is used to build up a theoretical model of plasma processing and to simulate the effect of pressure on the plasma density [11]. Although the basic data for activation process is still limited, one-dimensional model is proposed to describe the argon plasma state in the function of plasma parameters such as RF-voltage, DC-bias, and pressure. **Figure 18(a)** illustrates this one-dimensional model of argon plasma. Ionization of argon is expected to concentrate at the vicinity of tool surface in **Figure 9**. As depicted in **Figure 18(b)**, a hot spot with high electron temperature or the plasma sheath is formed only at the vicinity of cathode table. Under this geometric configuration, the electron density distribution is calculated at each specified pressure. **Figure 19** depicts a variation of electron density distribution with increasing the argon pressure. This enhancement
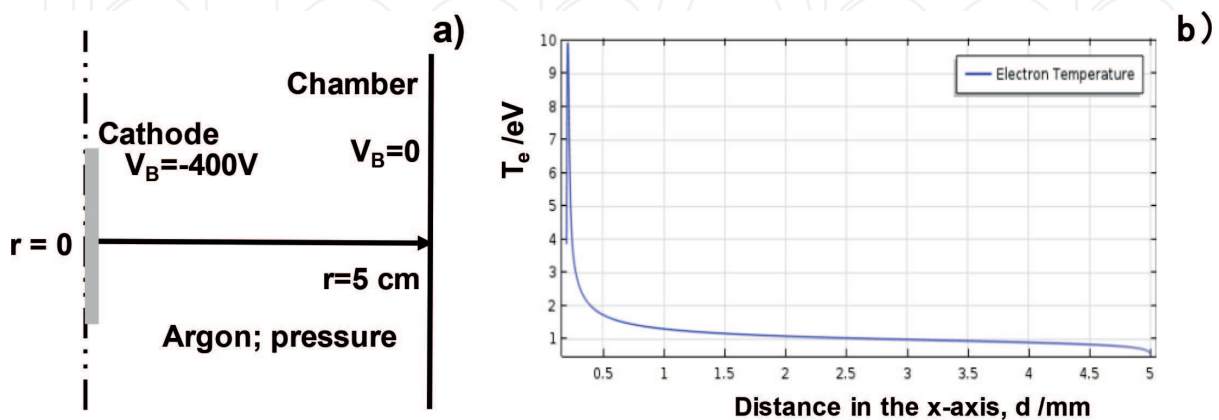
Figure 18. One dimensional model of argon plasma by using the multi-disciplinary equations. (a) Theoretical model of argon plasma, and, (b) decay of calculated electron temperature.
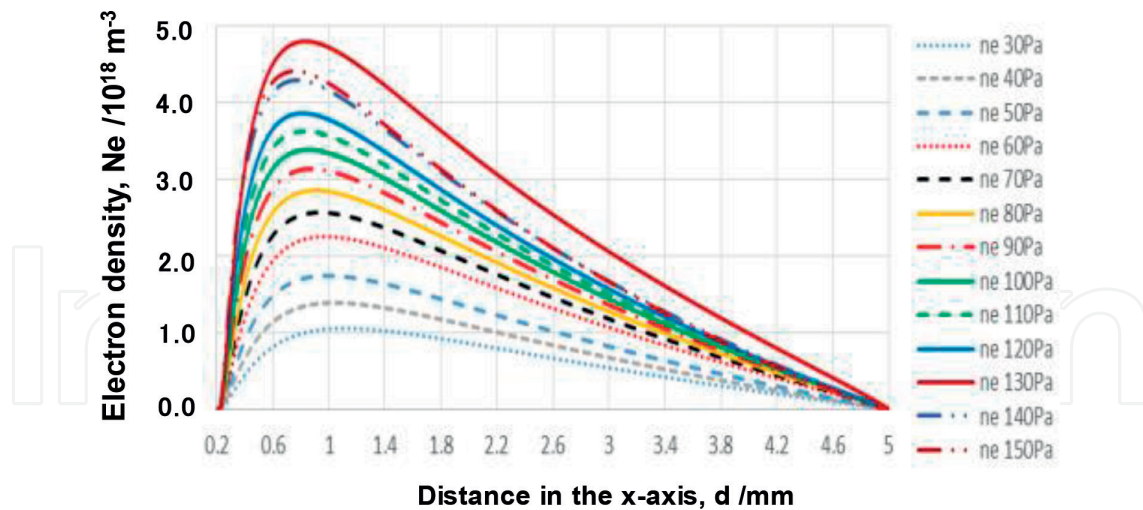
Figure 19. Enhancement of electron density distributions with increasing the argon pressure.

of electron density just near the cathode implies that electrons are activated in the plasma sheath. This theoretical model can be extended to describe the plasma oxidation process even by two dimensional model.

4.2. Down-sizing of plasma oxidation processing

Surface and interface area ratio to volume increases by down-sizing or miniaturing the dimensional size of products and elements. Surface or interface quality and functionality must be improved by surface- and interface -treatment and modification. The present plasma oxidation system has to be also down-sized to make plasma processing onto the surfaces and interfaces. **Figure 20(a)** illustrates a typical design of miniature plasma oxidation unit. RF-plasma is confined by using the RF-coils to form a plasma sheath around a small-sized tool above the insulator. The population of activated species in this plasma can be also controlled by the DC-bias. A shown in **Figure 20(b)**, a small-sized tool is subjected to high intensity plasmas in the designated space [18, 31].
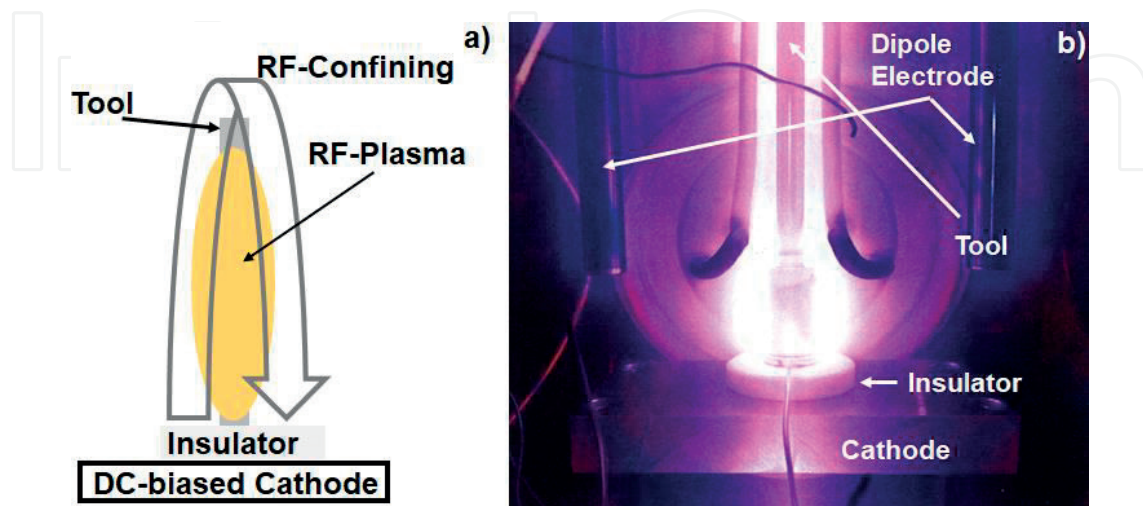

Figure 20. Down-sizing of an ashing unit for plasma oxidation of miniature parts and tools.

4.3. Plasma oxidation processing for industries

A single diamond-coated WC (Co) tool can be ashed away without residuals and tool edge damage by using the present plasma ashing system in **Figure 9**. Most of tooling companies are demanded to deal with hundreds of used diamond-coated tools in a day per a processing machine. The above plasma oxidation ashing system must be modified to make several or tens of works simultaneously even by using a single machine. The present system in **Figures 1** and **9** with use of the hollow cathode device is extended in the design concept to make simultaneous plasma oxidation for two diamond-coated tools [31, 32]. **Figure 21** depicts a developed simultaneous ashing system. The chamber is automatically opened for experimental set up of the diamond-coated tools, capped by the hollow cathode tubes.

An inserted photo in **Figure 21** shows that a pair of diamond-coated tool capped with the hollow cathode is subjected to the plasma oxidation. Only the inside of two hollows shines white; outside of hollows are in black. This reveals that oxygen plasmas are simultaneously confined into two hollows with high density and that ion density is much very low outside the hollows. This generation of oxygen plasmas is not limited to two hollows but extended to multi-ashing process to deal with tens of used diamond-coated tools by a single shot.
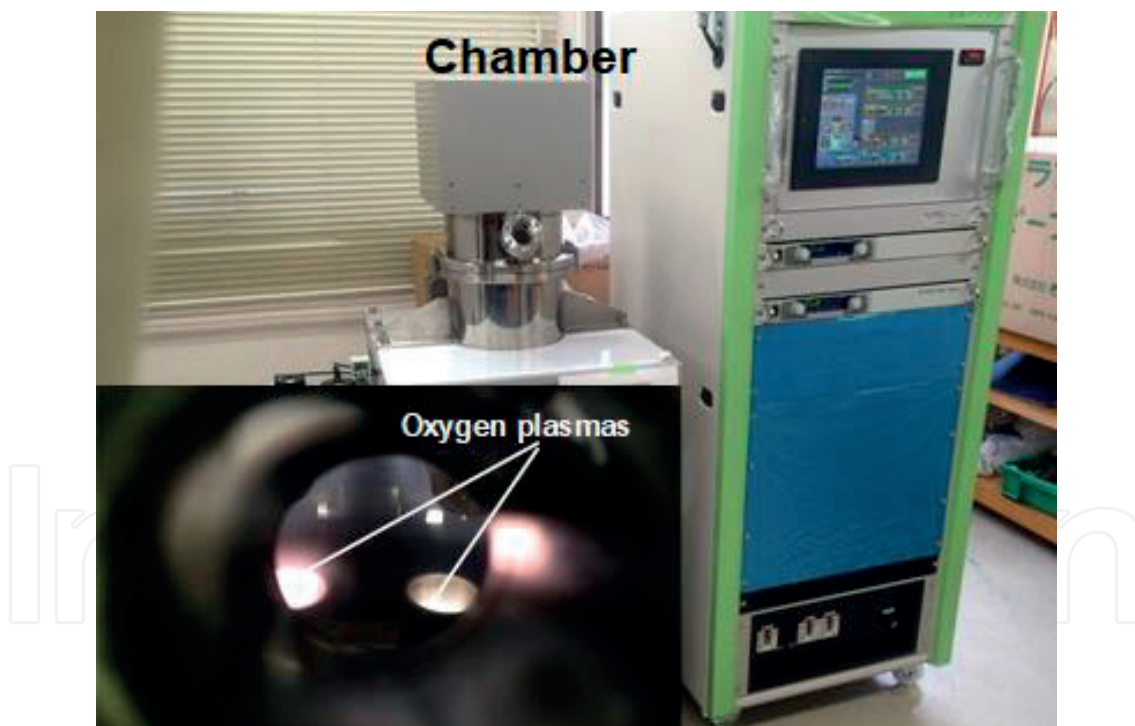
Figure 21. Simultaneous ashing system of two diamond-coated cutting tools toward industrial demonstration.

5. Conclusion

High density plasma oxidation ashing provides an effective processing to remove the used diamond films coated on the WC (Co) tool for recoating and reuse the mother tool substrate of WC

(Co). Different from the conventional plasma ashing processes in commercial, the diamond films are removed away without residuals even on the backsides of tool teeth and with less loss of teeth edges. In particular, the shrinkage in the tooth edge is more reduced down to 1.1 μm under the optimum ashing conditions than 5 μm in the commercial processes. In addition, the original microstructure with decobalted WC grains is reproduced by the present method to improve the engineering compatibility for nucleation and growth of diamond layers during the recoating process.

The emissive light optical spectroscopy as well as the Langmuir probe, equipped with the present system, work as a sensing medium to make quantitative diagnosis on the oxygen plasma state for optimization and to make in situ monitoring on the plasma oxidation reaction during the ashing process.

There might be several steps to extend this technology toward industrial applications. The carbon-base films including the diamond films are often utilized as a substrate of MEMS and miniature media; the small-scaled plasma ashing device is expected to work as a cutting and drilling tool to reshape that substrate and to modify its surface and interface. A miniatured oxygen plasma generator is just on the research to make demonstration tests. In practical operations of ashing processes in tooling industries, a stack of used diamond coated WC (Co) tools is processed by 100–1000 per a day. Considering that the tact time for present ashing is only 3.6 ks or 1 hour, tens of tools must be posttreated. The simultaneous plasma oxidation treatment is expected to be a candidate processing to make ashing of used diamond-coated tools in the industrial scale.

With aid of the theoretical model and simulation, the present plasma oxidation process can be extended to etching, polishing and finishing of various carbon base films, substrates and solid products by using the tailored devices to each application.

Acknowledgements

Conflict of interest

No conflict of interest was declared.

Author details

Tatsuhiko Aizawa

Address all correspondence to: taizawa@sic.shibaura-it.ac.jp

Surface Engineering and Design Laboratory, Shibaura Institute of Technology, Tokyo, Japan

References

[1] Hasegawa R. Cutting tools for aircraft and application. Journal of the Japan Society for Precision Engineering. 2009;**75**(8):953-957

[2] Bhushan B. Nano-tribology and nano-mechanics of MEMS/NEMS and bioMEMS/ bioNEMS material and device. Microelectronic Engineering. 2007;**84**:387-412

[3] Kohn E, Gluche P, et al. Diamond MEMS, a new emerging technology. Diamond and Related Materials. 1999;**8**:934-940

[4] Kurita T et al. Advanced material processing with nano- and femto- second pulsed laser. International Journal of Machine Tools and Manufacture. 2008;**48**:220-227

[5] Allen DM et al. Ion beam, focused ion beam, and plasma discharge machining. Manufacturing Technology. 2009;**58**:647-662

[6] Syrkin A et al. Reactive ion etching of 6H-SiC in an ECR plasma of CF4 -O2 mixture using both Ni and Al mask. Materials Science and Engineering. 1997;**B46**:374-378

[7] Aizawa T, Sugita Y. High-density plasma technology for etching and ashing of carbon materials. Research Reports SIT. 2011;**55**(2):13-22

[8] Aizawa T, Mizushima K, Redatiiono TN, Yang M. Micro-imprinting onto DLC and CNT coatings via high density oxygen plasma etching. In: Proc. 8th ICOMM Conference (Canada, Victoria); 2013. pp. 459-466

[9] Yamauchi K, Yunata EE, Aizawa T. High density oxygen plasma ashing of used CVD diamond coating for recycling of WC (Co) tools. In: Proc. 4th IFMM & IFBF (2015, Toyama); pp. 233-236

[10] Yunata EE, Aizawa T. Micro-texturing into DLC/diamond coated molds and dies via high density oxygen plasma etching. Manufacturing Review. 2015;**2**:1-8

[11] Yunata EE. Characterization and application of hollow cathode oxygen plasma [PhD. thesis]. Shibaura Institute of Technology; 2016

[12] Aizawa T. Micro-patterning onto diamond like carbon coating via RF-DC oxygen plasma etching. In: Proc. 8th SEATUC Conference (Vietnam, Hanoi); 2011. pp. 425-428

[13] Aizawa T, Fukuda T. Micro-texturing onto carbon-based coatings via oxygen plasma etching. Research Reports SIT. 2012;**56**(29):66-73

[14] Suenaga R, Yunata EE, Aizawa T. Quantitative plasma diagnosis on high density RF-DC plasmas for surface processing. In: Proc. 7th SEATUC Conference OS6 19; 2013. pp. 1-6

[15] Cvelbar U et al. Inductively coupled RF oxygen plasma characterization by optical emission spectroscopy. Vacuum. 2008;**82**:224-227

[16] Aizawa T, Fukuda T. Oxygen plasma etching of diamond-like carbon coated mold-die for micro-texturing. Surface and Coating Technology. 2013;**215**:364-368

[17]   Aizawa T, Morita H, Kurozumi S. Synthesis of films, coating system, coated products, dies and tools. In: Japanese Patent 2011-208140. 2011

[18]   Aizawa T, Sugita Y. Distributed nitriding systems for surface treatment of miniature functional products. In: Proc. 10th 4M/ICOMM; 2015. pp. 449-453

[19]   Bardos L. Radio frequency hollow cathodes for the plasma processing technology. Surface and Coating Technology. 1996;**46**:648-656

[20]   Kitano A. The CFRP which supports the light-weighting of the plane. Journal of Chemical Education. 2011;**59**(4):226-229

[21]   Aizawa T, Sugita Y. High density oxygen plasma ashing for recycling and reuse of DLC-coated tools and dies. Research Reports SIT. 2014;**58**(2):1-10

[22]   A. Gilpin, Composite Drill; Tool Process Change Nets 450 Percent More Holes per Bit Life. http://www.diamondtc.com/media/tooling_production/index.html [21/4/2018]

[23]   Aizawa T, Masaki E, Sugita Y. Oxygen plasma ashing of used DLC coating for reuse of milling and cutting tools. In: Proc. Int. Conf. Mater; Advanced Process Technology; 2011. pp. 15-20

[24]   Aizawa T, Masaki E, Sugita Y. Complete ashing of used DLC coating for reuse of the end-milling tools. Manufacturing Letters. 2014;**2**:1-3

[25]   Aizawa T, Masaki E, Moromoto E, Sugita Y. Recycling of DLC-coated tools for dry machining of aluminium alloys via oxygen plasma ashing. Mechanical Engineering Research. 2014;**4**(1):52-62

[26]   Yamauchi K, Aizawa T. Optimization of diamond ashing process for recoating of CVD diamond coated tools. In: Proc. 8th AWMFT; 2015. pp. J16/1-J16/6

[27]   Yunata EE, Yamauchi K, Aizawa T. High density plasma ashing of CVD diamond coated end-milling tools. In: Pro. 4th ASMP2015 (Lombok, Indonesia) 2015: CD-ROM

[28]   Yamauchi K, AizawaT. High density plasma ashing of used diamond coated short-shank tools without damage to WC (Co) teeth. In: Proc. 11th ICOMM 6; 2015. pp. 1-6

[29]   Mihailova D, Grozeva M, et al. Theoretical and experimental studies of the plasma processes in hollow cathode discharge lasers. In: Proc. 28th ICPIG, 98; 2007. pp. 533-536

[30]   Hagelaar GJM, Pitchford LC. Solving the Boltzmann equation to obtain electron transport coefficients and rate coefficients for fluid models. Plasma Sources Science and Technology. 2005;**14**:722-733

[31]   Aizawa T. Development of micro-manufacturing by controlled plasma technologies. Journal of Japan Society for Technology of Plasticity. 2017;**58**(12):1064-1068

[32]   Aizawa T. Future prospects and advanced steps of die and mold technologies. Journal of Japan Society for Technology of Plasticity. 2018;**59**(1):19-23